Quasi Z-Source Direct Matrix Converter for Enhanced Resilience to Power Grid Faults in Permanent Magnet Synchronous Motor Applications

Przemysław Siwek[1], Konrad Urbański[1]

[1] Poznan University of Technology, Institute of Robotics and Machine Intelligence, Piotrowo 3A, 60-965 Poznań

Abstract.. In this paper, a voltage control system for a PMSM motor based on the QZSDMC converter is proposed, which allows operation in both buck and boost modes as a possible method to make the drive resistant to power grid voltage sags. The authors presented a method for measuring and transforming the output voltage from QZS, enabling the use of a PI controller to control the voltage supplied to the DMC converter. The publication includes simulation and experimental studies comparing the operation of a PMSM motor powered by DMC and the proposed QZSDMC with voltage regulation. Simulation studies confirm the drive with QZSDMC resistance to voltage sags up to 80% of the rated value. Experimental studies demonstrate the correct operation of PMSM even with a power grid voltage amplitude equal to 40% of the rated value.

Key words: Permanent Magnet Synchronous Motor; Quasi Z-Source Direct Matrix Converter; Voltage Sag; Speed Control; Fault Tolerance

1. INTRODUCTION

With the increasing diversification of electric power sources and growing demand for it, the number of devices connected to the power grid increases every year. The continuous expansion of the grid and its decentralization result in an increased likelihood of occurrences of faults leading to a decrease in the quality of supplied voltage. Such events have a negative impact on both network users and electricity suppliers. Therefore, transmission and distribution system operators make every effort to ensure that the delivered electrical energy meets rigorous quality standards. Unfortunately, even the best-protected system can fail. Depending on the devices used and their applications, voltage disturbances in the network can cause shutdowns or malfunctions. These events result in real financial losses, the magnitude of which depends on the application and the protection measures employed. Therefore, the issue of damage to the power grid should be addressed not only by electricity suppliers but also by equipment manufacturers and network users. Users bear full responsibility for using devices safely and in accordance with their intended purpose, while manufacturers of electrical equipment are responsible for designing devices sold to exhibit high resilience to network faults.

Work on increasing the reliability of the electrical network and connected devices should begin with identifying the most common electrical disturbances. In [1], the electrical environment was described using three power quality surveys conducted in the United States of America and Canada. The authors chose this publication due to its detailed description of the frequency of occurrence of various types of electrical events.

In the industry, one of the most common loads encountered is electric motors. Among these motors, Permanent Magnet Synchronous Motors (PMSM) stand out due to their excellent dynamic performance, low inertia, high power density, and high efficiency, making them popular for demanding applications, with their control methods continually evolving [2, 3]. Nowadays, due to the drastic decrease in the cost of control electronics, power converters are utilized in applications with PMSM motors. Energy efficiency requirements encourage manufacturers to research the bi-directional power flow capability of servomotors. Hence, various converter topologies are being studied to find replacements for those currently available on the market. A Matrix Converter (MC) is an AC-AC converter containing an array of bi-directional switches, capable of connecting each load phase to any source phase [4, 5]. It offers several advantages over traditional converters, such as sinusoidal input and output currents, bi-directional power flow, and unity power factor. However, its drawback includes reduced output voltage to 0.866 times the supply voltage and susceptibility to network voltage quality deterioration and damage.

Matrix Converters (MC) are gaining popularity, among other applications, in wind turbines as converters capable of

supplying and receiving energy from the generator without any changes. This interest also extends to research related to the operation of MCs under network fault conditions. For example, in [6, 7], Fault Ride Through was utilized to enhance the resilience of matrix converters in wind turbine systems to network faults. Additionally, this converter is employed as one of the additional protective elements for larger systems. In [8], a single-phase MC was used to create a Dynamic Voltage Restorer (DVR) system compensating for voltage fluctuations in one phase of the network.

Despite their advantages, matrix converters have not yet replaced conventional solutions. One reason for this may be the lower output voltage of the converter compared to its input voltage. This issue was attempted to be addressed based on the works of Fang Zheng Peng, who described the Z-Source buck-boost inverter (ZS) in [9], a device enabling DC-AC, AC-DC, AC-AC, and DC-DC power conversion. Additionally, in [10], the Quasi Z-Source Inverter (QZS) was proposed, which partially addressed the problems of the previous device. The first combination of Peng's concepts with matrix converters was seen in work [11], where a new family of converters was introduced, named single-phase Z-source buck-boost Matrix Converters (ZSMC), and in [12], which extended the presented solution to the three-phase case.

The developed converters started to be investigated for their potential use of voltage boost to create devices resilient to faults or mitigate the impact of electrical network faults. In [18], the possibility of using ZSMC to increase the voltage at the load during voltage drops in the grid was presented. Unfortunately, the publication did not demonstrate a device operating automatically. In [19], a single-phase QZS was used to create a Dynamic Voltage Restorer (DVR) system compensating for voltage fluctuations in one phase of the network.

In the following paper, the application of voltage boost of QZSDMC was proposed to improve the safety of the control system against electrical network faults causing voltage sag. The authors adopted two assumptions regarding the device. The first is the operation of the converter without human supervision. The control system should automatically adapt to external events without causing error propagation to the motor load. The second is the ability to operate continuously in a fault state. The user has no influence on the duration of the voltage sag, and from a safety standpoint, the device should be able to operate for any length of time with voltage lower than nominal.

2. GRID FAULTS

Electrical networks, due to their size, number of elements, and complexity of the entire system, are susceptible to events such as faults or human errors. From the standpoint of loads, these events most commonly involve network voltage. These voltage events can be described by the magnitude of the voltage and the duration of their occurrence. It is assumed that they can last from milliseconds to hours [20].

In [1], the authors categorized voltage events based on their duration into:

- Transient Disturbances: These include unipolar transients, oscillatory transients (such as capacitor switching),

localized faults, and other events typically lasting less than 10 ms.
- Momentary Disturbances: These are voltage increases or decreases (sags, swells, and interruptions) lasting more than 10 ms but less than 3 s.
- Steady-State Disturbances: These are voltage increases or decreases (undervoltages, overvoltages, and interruptions) that last 3 s or longer.

In this paper, the focus is on the impact of voltage supplied to the load being lower than the nominal voltage. The most commonly used term for such an event is voltage sag. The authors [20] referred to its definition as: "short duration reductions in RMS voltage, caused by short circuits, overloads, and starting of large motors." This means that they occur as a result of events in the transmission system, which may be even hundreds of kilometers away from the affected load.

The magnitude of voltage sags is determined by several factors [20], including:

- Distance to fault,
- Cross section of the lines and cables,
- Connection type of transformers between the location of fault and the recording point,
- Type of the network (radial or loops),
- Short-circuit impedance of the network, etc

A single electrical event, depending on its occurrence point, applied protections, and the location of measurement, can yield different results during its examination. These differences are illustrated in Fig. 1. In the presented example, the voltage on the faulted feeder will drop to zero, while the voltage on the non-faulted feeder will drop to a nonzero value.
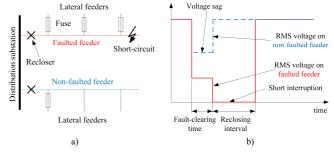

Fig.1. Fault in a distribution network: a) network layout and b) RMS voltages on feeders [20]

To determine the scope of research for this publication, data obtained in the United States of America and Canada were analyzed. These countries were chosen because a very comprehensive investigation regarding power quality for the US and Canada was conducted by a study based on three surveys carried out by the National Power Laboratory (NPL), the Canadian Electrical Association (CEA), and the Electric Power Research Institute (EPRI) [1]. Each organization collected measurement data at a different point. NPL examined voltages at electrical outlets, EPRI at substations, and CEA at service entrance panels. Due to the measurement points during the study, the authors considered data from CEA to be the most interesting for this publication. Therefore, further analyses are based on them.
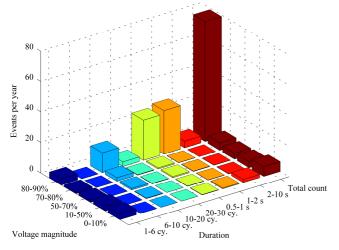
In 1991, the Canadian Electrical Association (CEA) initiated a three-year survey on power quality [21]. The primary objectives

of the survey were to assess the overall levels of power quality in Canada. The results would establish a baseline against which future surveys could be compared to identify trends. Twenty-two utilities across Canada participated in the survey, with a total of 550 sites monitored for 25 days each.

Residential, commercial, and industrial customer sites were monitored at their 120- or 347-V service entrance panels. Monitoring was conducted at the service entrance panel because it was deemed to provide a blended average of the power quality throughout the customer's premises. The CEA concluded that monitoring further into the premises might have unduly influenced the results by electrical loads on individual branch circuits, while monitoring at the distribution feeder would not have revealed disturbances originating within the customer's premises. Only line-to-neutral voltages were monitored, and both steady-state and triggered events were captured.
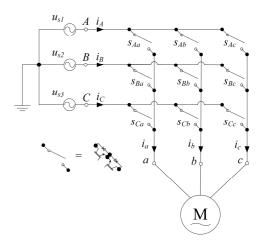
The data presented depict the occurrences of specific voltage events within one year (Fig. 2). The complete results included interruptions, voltage sags, and overvoltages. For the purposes of this publication, overvoltages were omitted. The data were divided based on voltage magnitude, indicating the level to which the measured voltage dropped, and on the duration of the event, which was categorized by the number of cycles/second of the event. From the presented data, it is evident that voltage sags of small magnitude predominated (80-90%). These events constituted 80% of all disturbances. It can also be observed that the majority of them lasted from 0.5 s to 2 s. In this publication, the decision was made to focus on voltage sags with a magnitude of 80% and a duration of 1 s.

Fig.2. Comparable events per year for CEA secondary-side data with no filter. Figure based on [1]

3. DIRECT MATRIX CONVERTER

A Direct Matrix Converter (DMC) is a type of power converter that does not have a voltage rectification stage in the output voltage modulation. Such a converter can be successfully utilized in servo motor systems. It consists of a grid filter to ensure device stability and a matrix of power electronic switches enabling bidirectional current flow. These switches can connect any phase of the grid to any phase of the load. A DMC without a grid filter is depicted in Fig. 3.

Fig.3. DMC topology

For correct operation, two rules must be introduced. Firstly, neither of the two input terminals must be connected to the same output phase to avoid source short circuits. Secondly, no output phase must be left open-circuited to prevent overvoltage caused by inductive loads. This limits the number of allowed switches configurations (active vectors) to 18 and zero configurations (zero vectors) to 3. Active and zero vectors can be found in works [22-24].

The Field Oriented Control (FOC) algorithm is based on dividing the three-phase motor current into two independent components: the i_d current generating the magnetic flux and the i_q current generating the torque. This simplifies the control of a three-phase motor to the control of flux and torque separately. This approach has been successfully adapted from Voltage Source Inverters to Matrix Converters [25]. The MC-FOC method enables the synthesis of the output voltage U_o by utilizing two neighboring active MC vectors. Due to the ability to connect any source phase with any load phase, the MC allows for control of the input current in the system. The synthesis method of the input current vector is the same as in the case of the output voltage (Fig. 4).
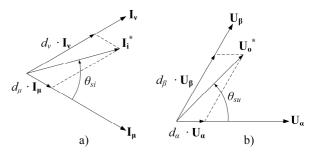

Fig.4. MC vector synthesis a) input current, b) output voltage

Using the law of sines, one can calculate the duty ratio of active and zero vectors according to the following formulas:

$$d_\alpha = \frac{T_\alpha}{T_s} = m_u \sin(60° - \theta_{su}),$$

$$d_\beta = \frac{T_\beta}{T_s} = m_u \sin(\theta_{su}), \qquad (1)$$

3

$$d_{0u} = \frac{T_{0u}}{T_s} = 1 - d_\alpha - d_\beta,$$

$$d_\mu = \frac{T_\mu}{T_s} = m_i \sin(60° - i),$$

$$d_v = \frac{T_v}{T_s} = m_i \sin(\theta_{si}), \qquad (2)$$

$$d_{0i} = \frac{T_{0i}}{T_s} = 1 - d_\mu - d_v,$$

where $T_x, x = \alpha, \beta, 0u, \mu, v, 0i$ describes the duration of an active or zero vector in a single time period T_s of converter operation, m_u describes the modulation index of output voltage and m_i is the modulation index of the input current.
Modulation indexes should be within the following ranges [25]:

$$0 \le m_u = \sqrt{3}\frac{|V_o|}{V_s} \le 1 \qquad (3)$$

$$0 \le m_i = \frac{|I_i|}{I_m} \le 1 \qquad (4)$$

where V_s is amplitude of grid voltage and I_m is RMS motor current. In order to simplify the further considerations, we assume that $m = m_u$. The next step is to combine both output voltage (1) and input current (2) modulation to get four pairs of the active vectors and one zero vector:

$$d_{\alpha\mu} = d_\alpha d_\mu = m \sin(60° - \theta_{sv}) \sin(60° - \theta_{sc})$$

$$d_{\beta\mu} = d_\beta d_\mu = m \sin(\theta_{sv}) \sin(60° - \theta_{sc})$$

$$d_{\alpha v} = d_\alpha d_v = m \sin(60° - \theta_{sv}) \sin(\theta_{sc}) \qquad (5)$$

$$d_{\beta v} = d_\beta d_v = m \sin(\theta_{sv}) \sin(\theta_{sc})$$

$$d_0 = 1 - d_{\alpha\mu} - d_{\beta\mu} - d_{\alpha v} - d_{\beta v}$$

4. QUASI Z-SOURCE DIRECT MATRIX CONVERTER

The Quasi Z-Source Direct Matrix Converter is a type of AC/AC buck-boost converter that allows for raising and lowering the average voltage within one PWM period. QZSDMC utilizes the unchanged topology of DMC, to which a QZS is connected without any additional modifications. The QZS circuit is a boost-type circuit that supplies voltage equal to or higher than the grid voltage to the DMC converter, which operates as a buck converter controlling the average voltage from 0 to 0.866 times the voltage at the output of QZS. Enabling DMC operation in the QZSDMC system requires only minor changes in the modulation algorithm. The undeniable advantages of the described converter compared to DMC include the ability to raise the voltage at the load and greater resilience to short-term faults resulting from transistor commutation errors. Unfortunately, the device is built with a larger number of components, and it is impossible to utilize 100% PWM duty cycle when the converter is in boost mode. The researched converter, as presented in Fig. 5, comprises a traditional DMC connected to six inductors inductors (L_{A1}, L_{B1}, L_{C1}, L_{A2}, L_{B2}, L_{B2}) and six capacitors (C_{A1}, C_{B1}, C_{C1}, C_{A2},

C_{B2}, C_{B2}). Coils L_{A1}, L_{B1} and L_{C1} act as grid current buffers, preventing the existence of discontinuous input current. Coils L_{A2}, L_{B2} and L_{C2} act as current sources, supplying power to the QZS capacitors with a high voltage. To enable this, the use of three additional bidirectional switches is required, unlike the traditional Matrix Converter (S_A, S_B, S_C). These switches are employed to control the boost operation of QZS. During normal operation, all switches should be turned on or off simultaneously, and thus controlled by a single gating signal.
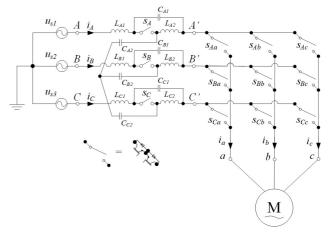

Fig.5. QZSDMC topology

According to [26], due to the converter's symmetry, the passive elements of QZS should have the same inductance and capacitance values. The QZSDMC converter operates in two states [28]. In the first state, known as Nonshoot-through (NST), switches S_{ABC} are turned on, allowing for a performance similar to traditional MC, conducting a voltage buck operation. In the second state, known as Shoot-through (ST), switches S_{ABC} are turned off, and switches S_{Aa}, S_{Ba}, S_{Ca} are turned on. It is important to note that the energy from QZS does not flow to MC due to the shorted outputs of the converter. Both states are depicted in Fig. 6. For one switching cycle T_S, the time interval of the ST state is T, and the time interval of NST state is T_1. Therefore, $T_S = T + T_1$, and the ST duty ratio is $D = T/T_S$. From Fig. 6, during the ST state, one can obtain the following voltage equations [28]:

$$\begin{bmatrix} u_{AB} \\ u_{BC} \\ u_{CA} \end{bmatrix} = \begin{bmatrix} u_{L_{A1}} \\ u_{L_{B1}} \\ u_{L_{C1}} \end{bmatrix} + \begin{bmatrix} u_{C_{A1}} \\ u_{C_{B1}} \\ u_{C_{C1}} \end{bmatrix} - \begin{bmatrix} u_{C_{B1}} \\ u_{C_{C1}} \\ u_{C_{A1}} \end{bmatrix} - \begin{bmatrix} u_{L_{B1}} \\ u_{L_{C1}} \\ u_{L_{A1}} \end{bmatrix} \quad (6)$$

where u_{AB}, u_{BC}, u_{CA} are phase to phase input voltages, u_{L_n} is voltage drop across inductor 1 in phase n, u_{C_n} is voltage drop across capacitor 1 in phase n. From Fig. 2, one can also derive the voltage equation for the NST state, which is given by the formula [28]:

$$\begin{bmatrix} u_{AB} \\ u_{BC} \\ u_{CA} \end{bmatrix} = \begin{bmatrix} u_{L_{A1}} \\ u_{L_{B1}} \\ u_{L_{C1}} \end{bmatrix} + \begin{bmatrix} u_{C_{A1}} \\ u_{C_{B1}} \\ u_{C_{C1}} \end{bmatrix} + \begin{bmatrix} u_{A'B'} \\ u_{B'C'} \\ u_{C'A'} \end{bmatrix} - \begin{bmatrix} u_{C_{B1}} \\ u_{C_{C1}} \\ u_{C_{A1}} \end{bmatrix} - \begin{bmatrix} u_{L_{B1}} \\ u_{L_{C1}} \\ u_{L_{A1}} \end{bmatrix} \quad (7)$$

In a steady state, the average voltage across the inductors in one switching cycle should be equal to zero, and from the symmetric voltages of the three-phase capacitors, we have [12]:

4

$$\begin{bmatrix} u_{A'B'} \\ u_{B'C'} \\ u_{C'A'} \end{bmatrix} = \frac{1}{1-2D} \begin{bmatrix} u_{AB} \\ u_{BC} \\ u_{CA} \end{bmatrix} \qquad (8)$$

In [12], boost factor for QZS was defined as:

$$B_{QZSDMC} = \frac{u_o}{u_i} = \frac{1}{1-2D} \qquad (9)$$

where u_i is the amplitude of input voltage and u_o is the output voltage amplitude of the QZS-network.
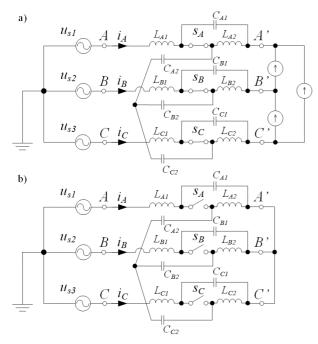

Fig.6. QZS circuits for a) Nonshoot-through and b) Shoot-through state

To utilize QZS with the Matrix Converter, one must select one of the voltage boost strategies. The simple boost strategy was described in [9]. Due to its simplicity, it can be implemented with minimal changes to the MC-FOC algorithm. This strategy involves introducing the ST state during the zero vector activity period when the motor phases are connected to a single power grid phase. Considering the above, the final form of the zero vector duration formula was derived:

$$d_0 = 1 - d_{\alpha\mu} - d_{\beta\mu} - d_{\alpha v} - d_{\beta v} - d_{ST} \qquad (10)$$

The sequence of control vectors' execution in a single period of converter operation was presented in Fig. 7, where V_k represents the active MC vector, and k is a ordinal number.
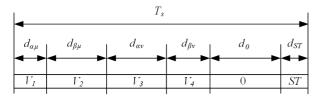

Fig.7. Switching sequence for the QZSDMC

5. CONTROL SYSTEM

The research employed a cascaded speed control system for driving PMSM. In this system, the speed controller calculates the reference value for the subordinate current control system. This setup is often used in industry due to its simplicity and well-established theoretical tuning principles. The motor current is controlled using the FOC method. The investigated control system, by utilizing QZS along with its controller, enables the control of the voltage reaching the DMC. The study compared the performance of a servo motor without QZS to the one containing it. The block diagram of the complete control system is depicted in Fig. 8.

The motor speed is controlled using the strategy of maintaining a constant power angle equal to $\pi/2$. This strategy involves keeping the i_d current equal to 0, thereby making the i_q current directly proportional to the motor's electrical torque. The current controllers had the same settings, calculated using the Modulus Optimum method. The speed controller was tuned using the Symmetrical Oprimum. All controllers used in the system had anti-windup mechanisms.
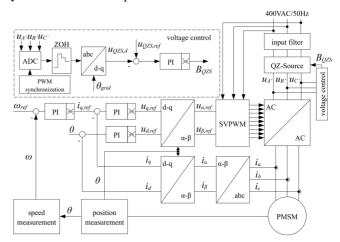

Fig.8. Block diagram of QZSDMC Field Oriented Control with voltage boost control

The control of the maximum voltage connected to the motor is achieved by setting the voltage gain value of the QZS system with a PI controller. The parameters of this controller were determined using optimization with the Hooke-Jeeves algorithm. The method of voltage measurement has a significant impact on the system's performance. Due to the nature of PWM operation, voltage measurement at the motor must be synchronized with its carrier signal period. Lack of synchronization can result in measurements equal to 0, with a higher likelihood as the duty cycle decreases. After gathering measurements, they are transformed using the abc-dq transformation with the rotation angle equal to the grid phase angle θ_{grid}. From these prepared voltage values, the error for the PI controller can be calculated. It's important to note that the QZS voltage control is fully automatic and does not require external information about grid faults. The described method is presented in Fig. 8.

The PMSM model used in the research was based on following equations:

5

$$T_e = \frac{3}{2}p\left[\Psi i_q + \left(L_d - L_q\right)i_d i_q\right] \qquad (11)$$

$$\frac{d}{dt}i_d = \frac{1}{L_d}u_d - \frac{R_s}{L_d}i_d + \frac{L_q}{L_d}p\omega i_q \qquad (12)$$

$$\frac{d}{dt}i_q = \frac{1}{L_q}u_q - \frac{R_s}{L_q}i_q - \frac{L_d}{L_q}p\omega i_d - \frac{\Psi p\omega}{L_q} \qquad (13)$$

$$\frac{d}{dt}\omega = \frac{1}{J}(T_e - T_m) \qquad (14)$$

where: T_e – electromagnetic torque, p – number of pole pairs, Ψ – permanent magnets flux linkage, L_d, L_q – d-q axis inductance, u_d, u_q – d-q axis voltages, R_s – stator resistance, ω – rotor angular velocity, J – inertia, T_m – load torque.

The parameters of the motors used in the simulation and real-world experiments differ. The ultimate goal of this publication is to present a system operating under industrial conditions. Therefore, the machine used in the simulation studies is a kilowatt-scale machine. In the experiments on the real-world system, due to the experimental nature of the converter allowing for voltage boosting and operation in short-circuit mode, a much smaller motor (Teknic M-2310P-LN-04K) was chosen. This approach is dictated by the cost of potential damage and machine replacement.

The QZS parameters used in the research were calculated based on [26]. A grid filter was added to improve system stability. Its structure and parameters were adopted from [27], where the cutoff frequency is arbitrarily determined. Typically, a frequency close to the PWM frequency is chosen.

The motor, RLC input filter and QZS parameters for simulation research are presented in Table 1 – 3.

TABLE 1. Rated parameters of PMSM

Parameter	Variable	Value
Inertia of rotor	J	0.0336 kgm^2
Permanent magnet flux	Ψ	0.5646 Wb
Stator resistance	R_s	3.55 Ω
d-axis inductance	L_d	17.16 mH
q-axis inductance	L_q	17.16 mH
Nominal speed	ω_N	157 rad/s

TABLE 2. Parameters of RLC input filter

Parameter	Variable	Value
RLC inductance	L_f	0.844 mH
RLC capacitance	C_f	0.3 µF
Damping capacitance	C_{PD}	1.2 µF
Damping resistance	R_f	53 Ω

TABLE 3. Parameters of QZS

Parameter	Variable	Value
QZS inductance	L_{ABC}	78 µH
QZS capacitance	C_{ABC}	1 µF

6. SIMULATION RESEARCH

A characteristic feature of the DMC is the connection of the grid phases to the load only through the filter. This design is susceptible to changes in grid voltage caused by electrical events, which are propagated to the powered device. This publication presents a control method for the QZSDMC converter that would enable the PMSM motor to operate with nominal parameters despite the occurrence of voltage sag in the grid. Any duration of the event was assumed here (from single cycles of grid voltage to an infinitely long time). This allows the proposed solution to be used at the ends of transmission lines, where the quality of the supplied voltage is low, and the line itself introduces a constant voltage drop, making it impossible for traditional servo motors to operate under nominal conditions. It can be assumed that such devices are desirable in places where user safety and resistance to external disturbances are important. In the actual research, it was decided to prove that the control system with QZSDMC under nominal conditions does not differ from the system with DMC.

The simulation research was conducted in the Matlab Simulink 2019a environment with the SimPowerSystems library. The models were designed to closely replicate real objects as much as possible. This was achieved by building converters from transistors, adding measurement noise, signal sampling (the control system operated with a period of 20 kHz), and adding parasitic parameters. The two studied systems differed only in the applied converter. The algorithms for selecting and calculating vector fill ratios were almost identical, except that in QZSDMC, the ST state was added during the duration of the zero vector.

The paper presents one simulation study confirming identical operation of the control systems under normal operating conditions and two studies demonstrating the behavior of the systems during power grid faults.

The first study depicts the operation of the control system with DMC and QZSDMC under normal operating conditions (Fig. 9). The study is divided into two parts. In the first part, the behavior of the devices is tested at rated speed and torque. The test begins with the motor accelerating from $\omega = 0$ rad/s to the rated speed $\omega = 157$ rad/s. Once the rated speed is reached, the load torque is applied. After 1 s from the start of the simulation, the set speed is set to -157 rad/s, causing the motor to decelerate. The simulation ends after 2.5 s with the motor rotating at negative speed. The current controllers operate in saturation, confirming constant acceleration of the motor during startup and deceleration.

In the second part of the first study, the behavior of the systems in the linear operating range was examined (Fig. 10). This was achieved by a step change in the speed reference value to 0.05 rad/s, applying the rated load torque, and then setting the reference speed back to zero after 0.1 s. When the current controllers do not saturate, the quality of speed control can be determined. In Fig. 10, it can be observed that the speed waveforms for both drives almost overlap. Therefore, it can be concluded that under rated voltage conditions, the converters behave identically even in the low-speed range.

6

The test was conducted to demonstrate the identity of the investigated control systems in terms of motor speed control in the linear range. Both models are so similar to each other that they are almost perfectly superimposed on the graphs. The quality index is also close to zero. Any differences may arise from the noise introduced into the system's speed and current measurements.
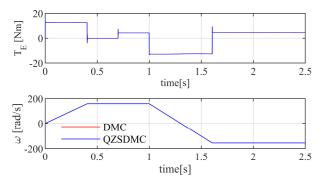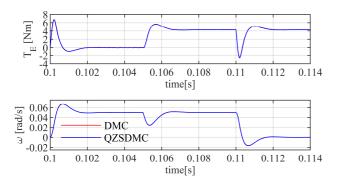

Fig.9. Nominal work of PMSM control system

Fig.10. Operation of the control system in the linear range

The second study aimed to demonstrate the impact of an 80% magnitude voltage sag in all three phases on the operation of the control systems with DMC and QZSDMC under nominal conditions with rated torque. There were no changes made to the control systems themselves except for the input voltage. The system was still subjected to the same load and had the same reference speed.

The purpose of the study was to determine whether the use of QZSDMC to compensate for voltage fluctuations at the motor could increase the system's resilience to electrical events causing voltage sag. Additionally, it was examined whether it is possible to achieve the rated voltage at the motor when the voltage drop on the power grid is too significant for the motor to rotate at the rated speed when powered by a traditional DMC. The phase-to-phase voltage of the grid along with the grid current for the QZSDMC system is illustrated in Fig. 11. As anticipated, after the voltage sag occurred at 0.5 s, the grid current increased. This is due to the voltage boost performed by QZS. The phase-to-phase voltage and the motor current supplied by DMC are depicted in Fig. 12. It can be observed that after the voltage sag, the converter cyclically enters states of continuous conduction, attempting to deliver a maximally high voltage to the load. However, despite this effort, the delivered voltage was too low to balance the EMF of the motor.

The PMSM began to decelerate after the voltage sag, leading to a transition to regenerative operation. This is evident in the figure as a change in sign and an increase in the amplitude of the motor current.
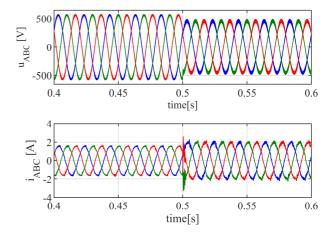

Fig.11. Grid phase to phase voltage and grid current during 80% 3-phase sag in QZSDMC control system
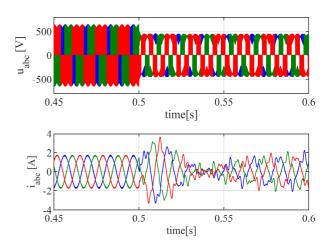

Fig.12. Voltage and current of PMSM fed by DMC during 80% 3-phase sag

Figure 13 illustrates the phase-to-phase voltage and the current of the machine powered by QZSDMC. After the voltage sag occurred, the control system requires 2 ms to react and regulate the voltage and current. Apart from this moment, the voltages and currents on the motor are nearly identical before and after the event.

7. EXPERIMENTAL RESEARCH

The experimental research was conducted on a compact setup featuring the Teknic M-2310P-LN-04K motor. This motor was powered by an experimental QZSDMC converter. The control algorithms and measurements were performed on the STM32H723ZG system, which can be classified as a low-cost solution, providing a clear advantage for practical applications. The motor, RLC input filter and QZS parameters of a prototype are presented in Table 4 – 6.
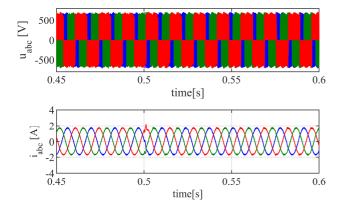
Fig.13. Voltage and current of PMSM fed by QZSDMC during 80% 3 phase sag

TABLE 4. Rated parameters of PMSM

Parameter	Variable	Value
Inertia of rotor	J	0.0006 kgm^2
Torque constant	K_t	0.0122 Nm/A
Stator resistance	R_s	0.72 Ω
d-axis inductance	L_d	40 mH
q-axis inductance	L_q	40 mH
Nominal speed	ω_N	628 rad/s

TABLE 5. Parameters of RLC input filter

Parameter	Variable	Value
RLC inductance	L_f	375 µH
RLC capacitance	C_f	0.3 µF
Damping capacitance	C_{PD}	1.2 µF
Damping resistance	R_f	35 Ω

TABLE 6. Parameters of QZS

Parameter	Variable	Value
QZS inductance	L_{ABC}	30 µH
QZS capacitance	C_{ABC}	10 µF

In the experimental investigations, emphasis was placed on measurable, practical effects of the converter's operation. Therefore, the step response of the voltage control system (u_{QZS}) and the motor's performance during voltage sag were examined. The first experimental study involved testing the operation of the voltage controller u_{QZS} (Fig. 14). In this study, the reference voltage was stepwise changed from 22.5 V to 37 V. Measurements were conducted at a frequency of 20 kHz using ADC converters embedded in the microcontroller. The result presented in Figure 14 is the average of 20 trials, where each resulting sample shown in the figure is the arithmetic mean of 20 synchronized samples relative to the step change of the reference value. This result enables the assessment of the repeatability of the entire control system's operation. For the presented data, the variance was 0.54 V, which corresponds to 1.5% of the voltage value after the step change. Additionally, it can be observed from the figure that the control system completed its operation in less than 1 ms. The visible oscillations are characteristic of the system's response.
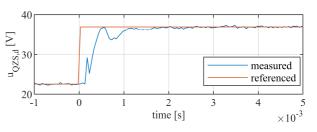

Fig.14. Step response of the $u_{QZS,d}$ voltage regulation system when the reference voltage changes from 22.5 V to 37 V

In the second experimental study, the operation of the QZSDMC and DMC converters during a voltage sag was examined. The study involved linearly reducing the grid voltage and determining at what voltage amplitude the PMSM motor would start to decelerate. During the tests, both systems operated in a closed-loop speed control configuration. Figure 15 illustrates the operation of the PMSM motor during a voltage sag in the DMC system. The presented data indicate that a decrease in the supply voltage amplitude by just 0.5 V results in a decrease in the machine's rotational speed. Initially, the difference is small; however, it can lead to errors in the operation of machines driven by such a servo motor.
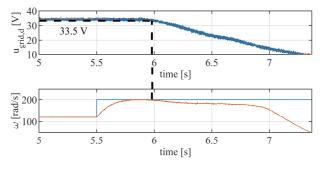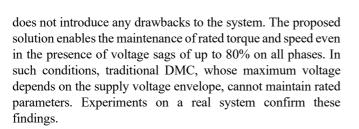

Fig.15. DMC and PMSM response to a linear decrease in grid voltage from 34 V to 10 V

Figure 16 depicts the QZSDMC system. The first plot includes the measured grid voltage, which starts to decrease at around 5.75 s until it reaches 10 V. The second plot shows the measured and desired rotational speed of the PMSM motor. It can be observed that despite the decrease in the supply voltage, the motor is able to maintain the desired speed. The speed began to decrease after exceeding 14.4 V. The third plot presents the desired voltage gain BQZS. It is evident that the voltage controller saturates when the amplitude of the grid voltage reaches approximately 20 V. This saturation depends on the current and voltage ratings of the converter components.

8. CONCLUSIONS

Disruption to the power grid has adverse consequences on all devices linked to it. The research cited indicates that such events occur on average several times a month. Therefore, industrial devices should be resilient to these disruptions. The paper proposes a method of controlling QZSDMC to improve the resilience of matrix converters to grid faults. The research suggests that from the perspective of the speed control loop, the control system with QZSDMC operates the same as with DMC under rated conditions. This means that adding QZS to DMC
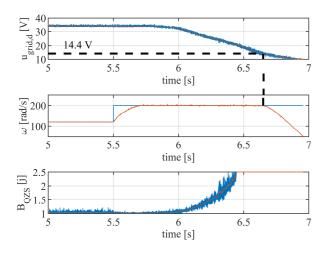
does not introduce any drawbacks to the system. The proposed solution enables the maintenance of rated torque and speed even in the presence of voltage sags of up to 80% on all phases. In such conditions, traditional DMC, whose maximum voltage depends on the supply voltage envelope, cannot maintain rated parameters. Experiments on a real system confirm these findings.

Fig.16. QZSDMC and PMSM response to a linear decrease in grid voltage from 34 V to 10 V with a closed-loop voltage control system

REFERENCES

[1] D. S. Dorr, T. M. Gruzs, M. B. Hughes, R. E. Jurewicz, Gurcharn Dang and J. L. McClaine, "Interpreting recent power quality surveys to define the electrical environment," IAS '96. Conference Record of the 1996 IEEE Industry Applications Conference Thirty-First IAS Annual Meeting, San Diego, CA, USA, 1996, pp. 2251-2258 vol.4.

[2] T. Tarczewski, R. Szczepanski, K. Erwinski, X. Hu and L. M. Grzesiak, "A Novel Sensitivity Analysis to Moment of Inertia and Load Variations for PMSM Drives," in IEEE Transactions on Power Electronics, vol. 37, no. 11, pp. 13299-13309, Nov. 2022, doi: 10.1109/TPEL.2022.3188404.

[3] M. Morawiec, A. Lewicki and I. C. Odeh, "Rotor-Flux Vector Based Observer of Interior Permanent Synchronous Machine," in IEEE Transactions on Industrial Electronics, vol. 71, no. 2, pp. 1399-1409, Feb. 2024, doi: 10.1109/TIE.2023.3250851.

[4] P. W. Wheeler, J. Rodriguez, J. C. Clare, L. Empringham and A. Weinstein, "Matrix converters: a technology review," in IEEE Transactions on Industrial Electronics, vol. 49, no. 2, pp. 276-288, Apr 2002.

[5] P. Szcześniak and J. Kaniewski, "Hybrid Transformer With Matrix Converter," in IEEE Transactions on Power Delivery, vol. 31, no. 3, pp. 1388-1396, June 2016, doi: 10.1109/TPWRD.2015.2493508.

[6] K. Inomata et al., "Enhanced fault ride through capability of matrix converter for wind power system," IECON 2013 - 39th Annual Conference of the IEEE Industrial Electronics Society, Vienna, 2013, pp. 4838-4843.

[7] H. Takahashi and J. Itoh, "Ride through capability of matrix converter for grid connected system under short voltage sag," IECON 2015 - 41st Annual Conference of the IEEE Industrial Electronics Society, Yokohama, 2015, pp. 005298-005303.

[8] K. Yamamoto, K. Ikeda, Y. Tsurusaki and M. Ikeda, "Characteristics of voltage sag/swell compensator utilizing single-phase matrix converter," 2013 International Conference on Electrical Machines and Systems (ICEMS), Busan, 2013, pp. 1863-1868.

[9] F. Z. Peng, "Z-source inverter," IEEE Trans. Ind. Appl., vol. 39, no. 2, pp. 504–510, Mar/Apr. 2003.

[10] J.Anderson and F. Z. Peng, "Four quasi-Z-source inverters," in Proc. IEEE Power Electron. Specialists Conf., Jun. 15–19, 2008, pp. 2743–2749.

[11] M. Nguyen, Y. Jung, Y. Lim and Y. Kim, "A Single-Phase Z-Source Buck–Boost Matrix Converter," in IEEE Transactions on Power Electronics, vol. 25, no. 2, pp. 453-462, Feb. 2010.

[12] B. Ge, Q. Lei, W. Qian and F. Z. Peng, "A Family of Z-Source Matrix Converters," in IEEE Transactions on Industrial Electronics, vol. 59, no. 1, pp. 35-46, Jan. 2012.

[13] S. Liu, B. Ge, X. Jiang, H. Abu-Rub, and F. Z. Peng, "Modeling, analysis, and motor drive application of quasi-Z-source indirect matrix converter," Int. J. Comput. Math. Electr. Electron. Eng., vol. 33, no. 1/2, pp. 298–319, 2014.

[14] S. Liu, B. Ge, X. You, X. Jiang, H. Abu-Rub, and F. Z. Peng, "A novel quasi-Z-source indirect matrix converter," Int. J. Circuit Theory Appl.,vol. 43, no. 4, pp. 438–454, Apr. 2015.

[15] O. Ellabban, H. Abu-Rub and S. Bayhan, "Z-Source Matrix Converter: An Overview," in IEEE Transactions on Power Electronics, vol. 31, no. 11, pp. 7436-7450, Nov. 2016.

[16] E. Karaman, M. Farasat and A. M. Trzynadlowski, "A Comparative Study of Series and Cascaded Z-Source Matrix Converters," in IEEE Transactions on Industrial Electronics, vol. 61, no. 10, pp. 5164-5173, Oct. 2014.

[17] S. Liu, B. Ge, X. Jiang, H. Abu-Rub and F. Z. Peng, "Comparative Evaluation of Three Z-Source/Quasi-Z-Source Indirect Matrix Converters," in IEEE Transactions on Industrial Electronics, vol. 62, no. 2, pp. 692-701, Feb. 2015.

[18] K. Park and K. Lee, "A Z-source sparse matrix converter under a voltage sag condition," 2010 IEEE Energy Conversion Congress and Exposition, Atlanta, GA, 2010, pp. 2893-2898.

[19] M. Trabelsi, P. Kakosimos and H. Komurcugil, "Mitigation of grid voltage disturbances using quasi-Z-source based dynamic voltage restorer," 2018 IEEE 12th International Conference on Compatibility, Power Electronics and Power Engineering (CPE-POWERENG 2018), Doha, 2018, pp. 1-6.

[20] F. Iov, D. A. Hansen, P. E. Sørensen, N. A. Cutululis, "Mapping of Grid Faults and Grid Codes", Roskilde: Risø National Laboratory. Denmark. Forskningscenter Risoe. Risoe-R, No. 1617(EN).

[21] M. B. Hughes and J. S. Chan, "Canadian National power quality survey results," in Proc. EPRI PQA'95, New York, NY, May 9–11, 1995.

[22] C. Xia, J. Zhao, Y. Yan and T. Shi, "A Novel Direct Torque Control of Matrix Converter-Fed PMSM Drives Using Duty Cycle Control for Torque Ripple Reduction," in IEEE Transactions on Industrial Electronics, vol. 61, no. 6, pp. 2700-2713, June 2014.

[23] P. Szczesniak, K. Urbanski, Z. Fedyczak, K. Zawirski, "Comparative study of drive systems using vector-controlled PMSM fed by a matrix converter and a conventional frequency converter," Turkish Journal of Electrical Engineering and Computer Sciences, 2016, 24. 1516-1531.

[24] D. Majchrzak and P. Siwek, "Comparison of FOC and DTC methods for a Matrix Converter-fed permanent magnet synchronous motor," 2017 22nd International Conference on Methods and Models in Automation and Robotics (MMAR), Miedzyzdroje, 2017, pp. 525-530.

[25] L. Huber and D. Borojevic, "Space vector modulated three-phase to three-phase matrix converter with input power factor correction," in IEEE Transactions on Industry Applications, vol. 31, no. 6, pp. 1234-1246, Nov/Dec 1995.

[26] S. Liu, B. Ge, Y. Liu, H. Abu-Rub, R. S. Balog and H. Sun, "Modeling, Analysis, and Parameters Design of LC-Filter-Integrated Quasi-Z - Source Indirect Matrix Converter," in IEEE Transactions on Power Electronics, vol. 31, no. 11, pp. 7544-7555, Nov. 2016.

[27] Bauer J., Fligl S., Steimel A., "Design and Dimensioning of Essential assive Components for the Matrix Converter Prototype," Automatika, vol. 53, no. 3, 2012, pp.225-235.

[28] O. Ellabban, H. Abu-Rub and B. Ge, "A Quasi-Z-Source Direct Matrix Converter Feeding a Vector Controlled Induction Motor Drive," in IEEE Journal of Emerging and Selected Topics in Power Electronics, vol. 3, no. 2, pp. 339-348, June 2015